

Supplemental Information for:

**Chemical Characterization of Polymer and Chloride Content in Waste Plastic
Materials Using Pyrolysis – Direct Analysis in Real Time – High-Resolution**

Mass Spectrometry

Emily Halpern,¹ Lauren Heirty,¹ Christopher West,¹ Yitao Li,² Won M. Kim,³ Anthony S. Mennito,³ Alexander Laskin.¹

¹*Department of Chemistry, Purdue University, West Lafayette, IN, 47907, USA.*

²*Department of Statistics, Purdue University, West Lafayette, IN, 47907, USA.*

³*ExxonMobil Technology and Engineering Company, Annandale, NJ, 08801, USA.*

Content

Figure S1: Monomeric KMD plots of PP and PS.

Figure S2: Evolution of KMD_{CH_2} of plastic reference materials with temperature in pyro-(+)DART-HRMS.

Figure S3: pyro-(+)DART-HRMS total ion chromatograms or thermograms of plastic reference materials

Figure S4: pyro-(-)DART-HRMS total ion chromatograms or thermograms of plastic reference materials

Figure S5: Evolution of KMD_{CH_2} of plastic reference materials with temperature in pyro-(-)DART-HRMS

Figure S6: pyro-(+)DART-HRMS temperature-separated MS plots of waste plastics

Figure S7: pyro-(+)DART Temperature-separated KMD_{CH_2} plots of waste plastics

Figure S8: pyro-(-)DART-HRMS temperature-separated MS plots of waste plastics

Figure S9: pyro-(-)DART Temperature-separated KMD_{CH_2} plots of waste plastics

Figure S10: KMD_{CH_2} plots with increasing standard additions of polyethylene to polystyrene.

Table S1: Results of statistical TC analysis with standard addition mixtures of plastic standards: polyethylene and polystyrene

Figure S11: KMD_{CH_2} plots with increasing standard additions of polypropylene to polystyrene.

Table S2: Results of statistical TC analysis with standard addition mixtures of plastic standards: polypropylene and polystyrene

Figure S12: KMD_{CH_2} plots with increasing standard additions of polystyrene to Waste A.

Table S3: Results of statistical TC analysis with standard addition mixtures of plastic standards: Waste A and polystyrene

Figure S13: Formula assignments of $\text{Cu}_x\text{Cl}_{x+1}^-$ peaks observed in the pyro-(–)DART-HRMS analysis of PVC

Figure S14: Isotopic distribution of observed $\text{Cu}_x\text{Cl}_{x+1}^-$ peaks compared to predicted isotope distribution.

Appendix A: Description of Tanimoto Coefficient Calculation for one Homologous Series

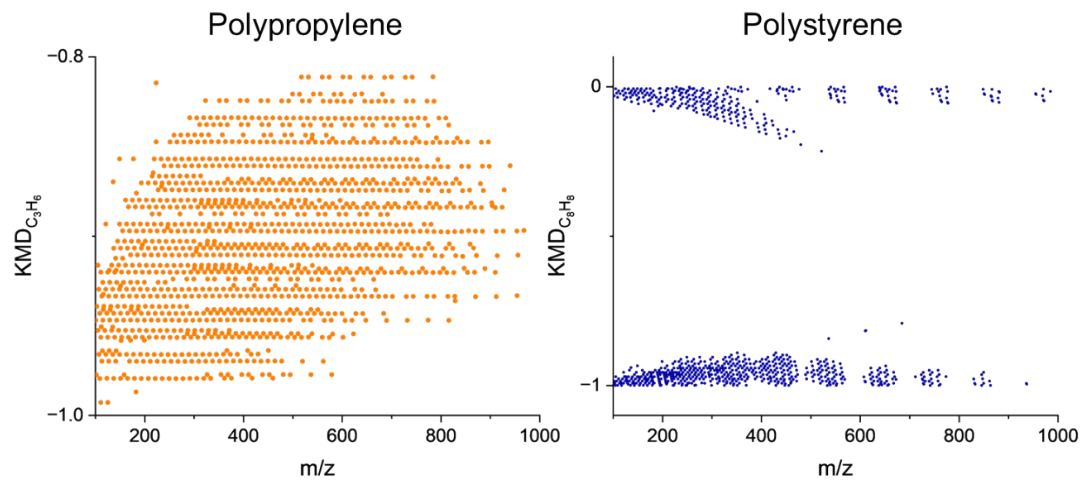


Figure S1: Monomeric KMD plots of polypropylene and polystyrene. Polypropylene is on the left with a C_3H_6 (propyl) Kendrick base applied and polystyrene is on the right with a C_8H_8 (styrene) Kendrick base applied.

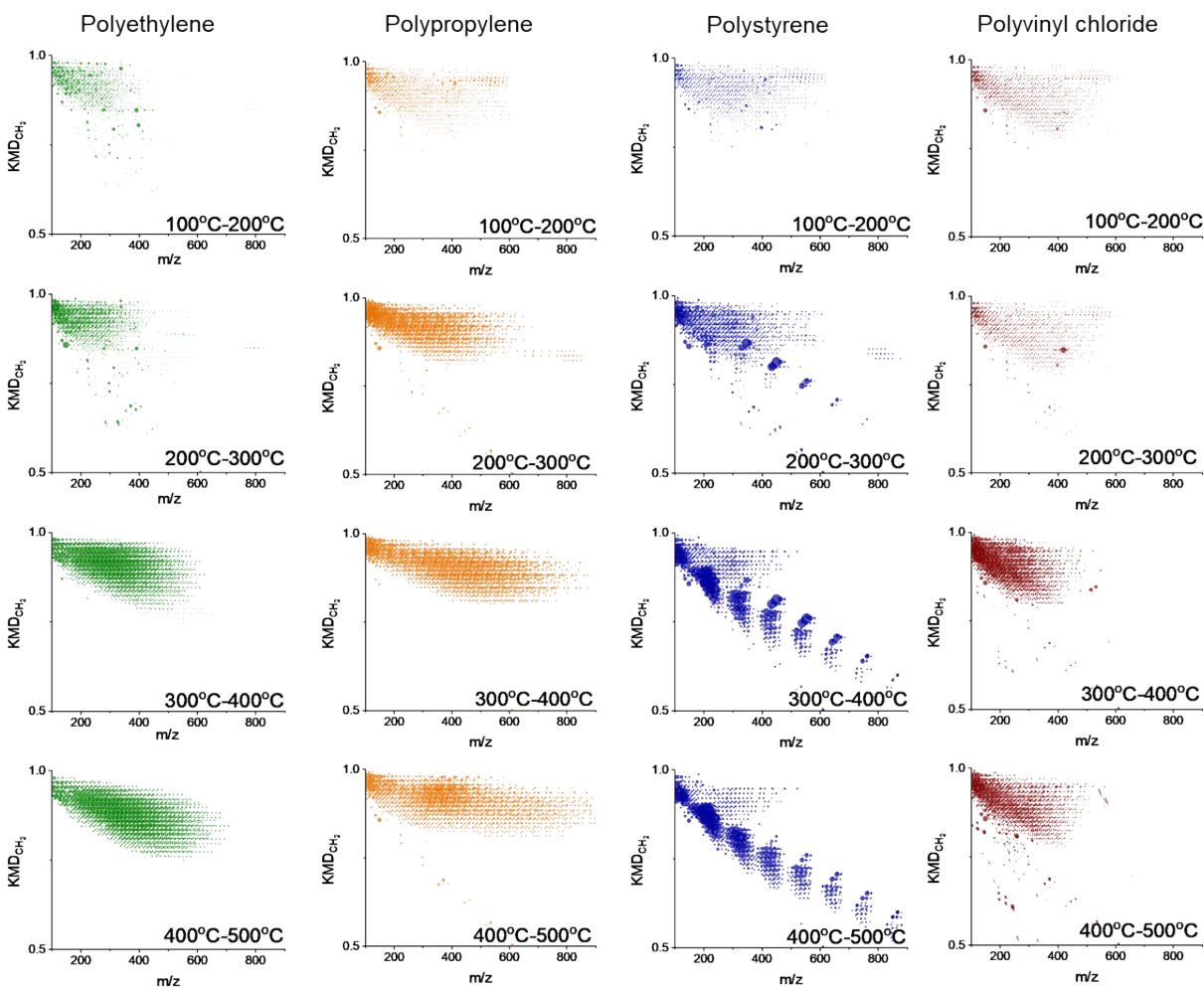


Figure S2: Evolution of CH₂-Kendrick mass defect plots of plastic reference materials summarized for increasing desorption temperatures in pyro-(+)DART-HRMS experiments. Individual points are scaled according to (intensity)^{1/3}. Higher molecular weight species appear as higher temperatures are applied.

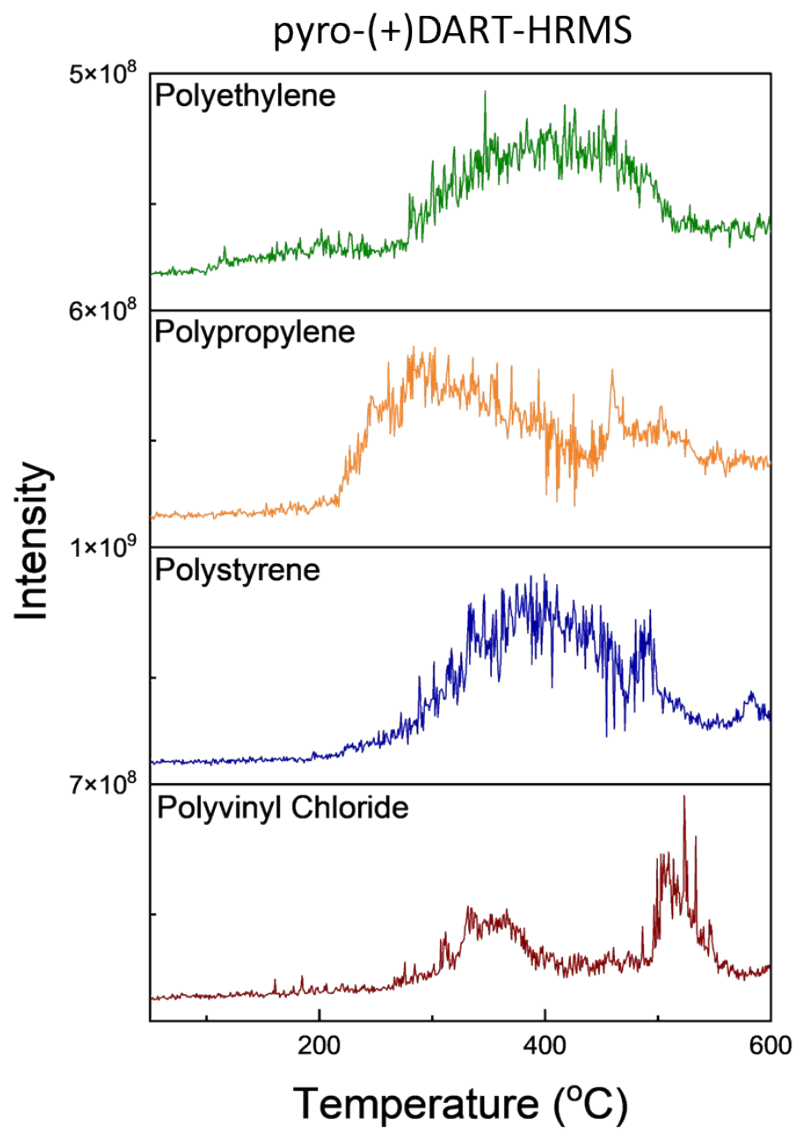


Figure S3: Total ion chromatograms/thermograms of plastic desorption of plastic reference materials in pyro-(+)DART-HRMS experiments.

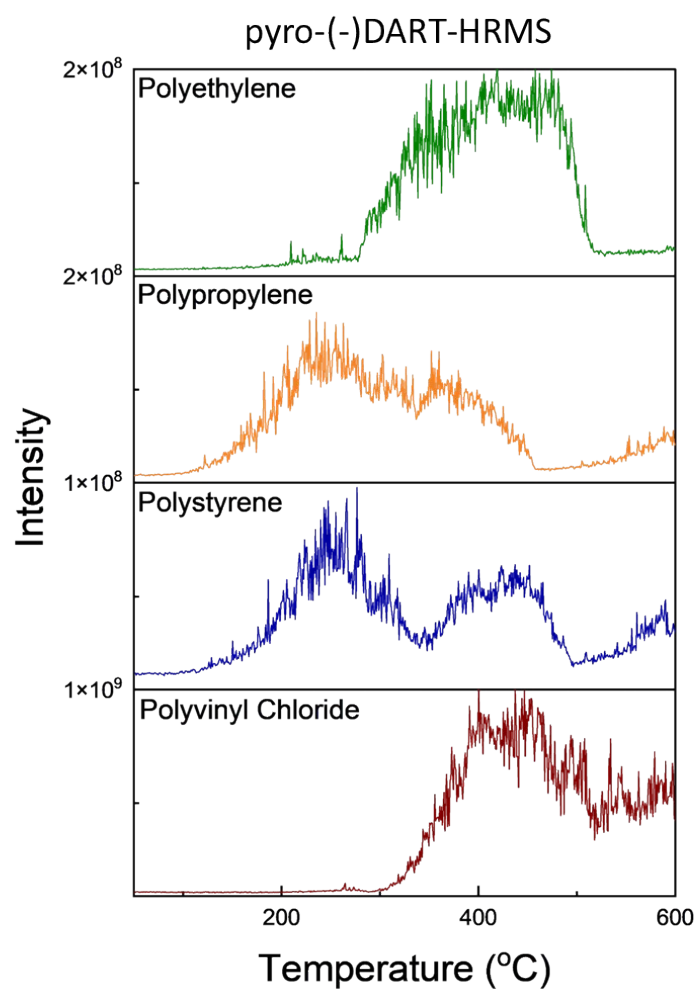


Figure S4: Total ion chromatograms/thermograms of plastic desorption of plastic reference materials in pyro(-)DART-HRMS experiments. Dechlorination products of PVC can be detected at temperatures as low as 300°C as depicted by the rapid increase in intensity at that temperature.

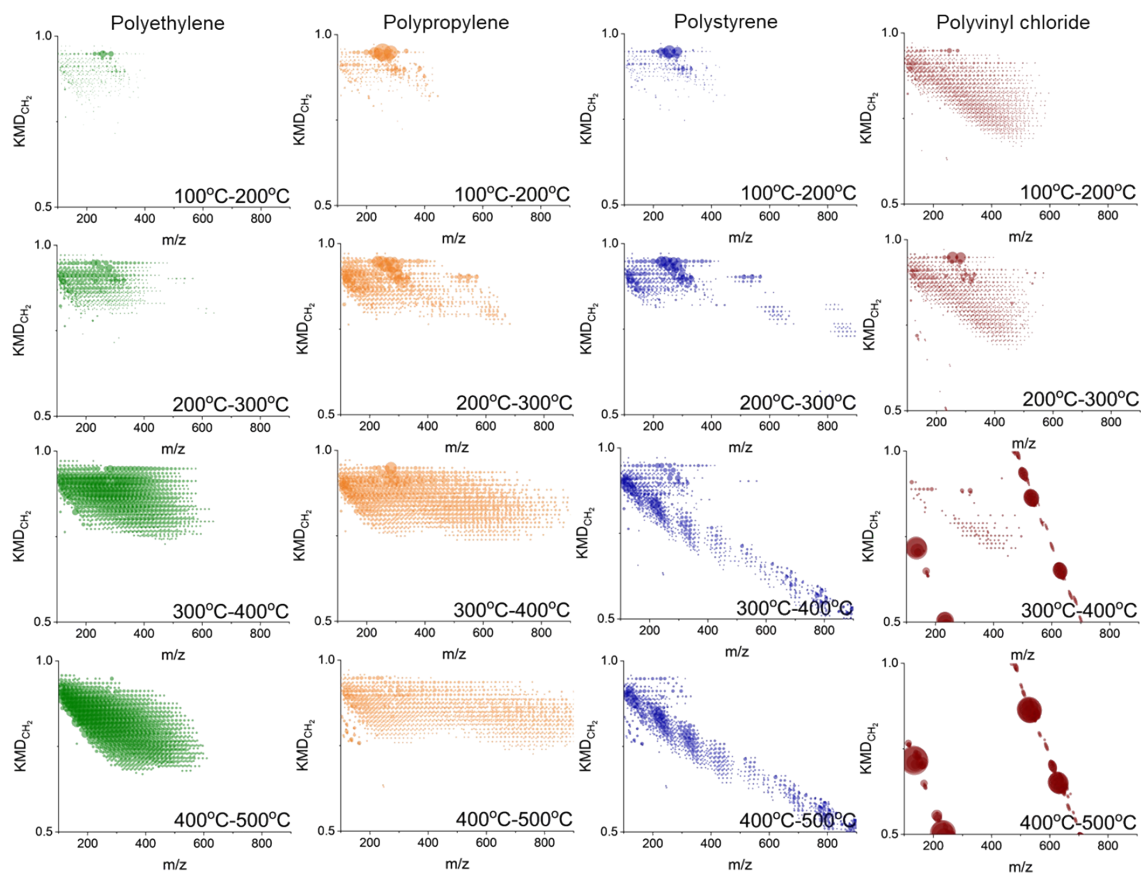


Figure S5: Evolution of CH₂-Kendrick mass defect plots of plastic reference materials summarized for increasing desorption temperatures in pyro(-)DART-HRMS experiments. Individual points are scaled according to (intensity)^{1/3}. Higher molecular weight species appear as higher temperatures are applied.

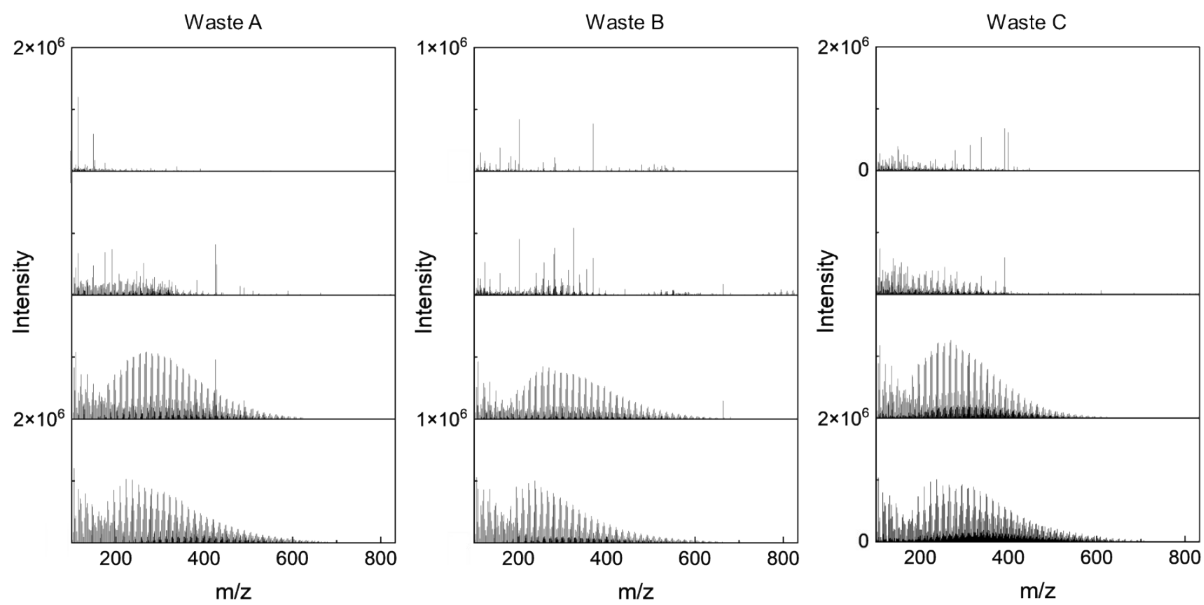


Figure S6: pyro-(+)DART-HRMS temperature-separated MS plots of waste plastics

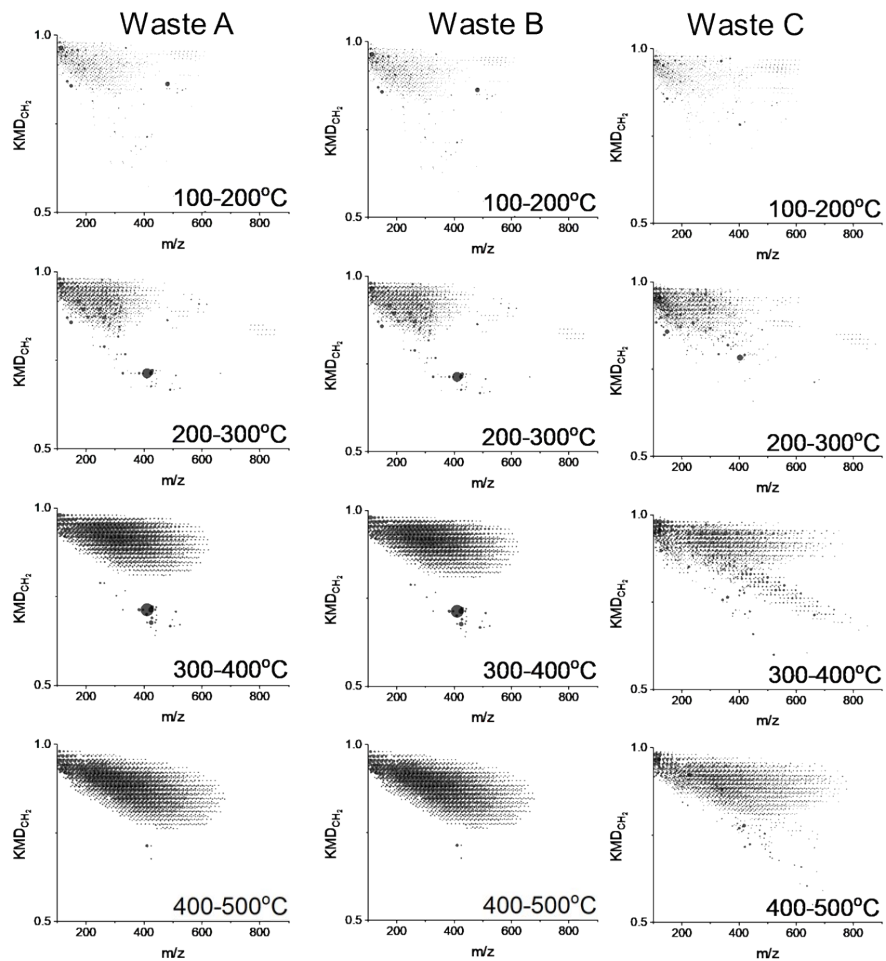


Figure S7: Evolution of CH₂-Kendrick mass defect plots of waste plastics summarized for increasing desorption temperatures in pyro-(+)DART-HRMS experiments. Individual points are scaled according to (intensity)^{1/3}.

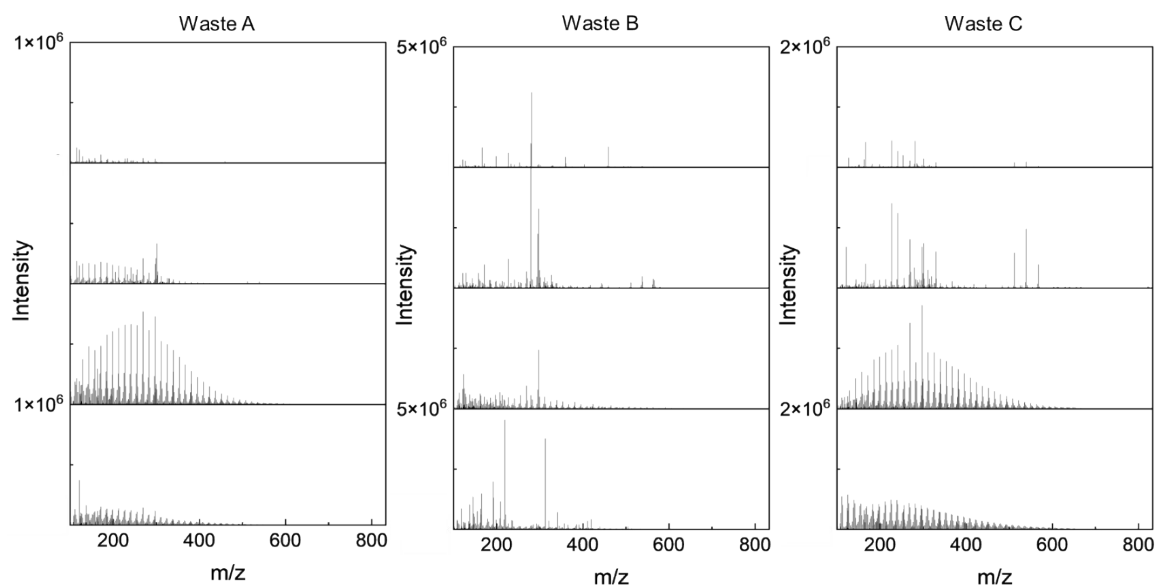


Figure S8: pyro-(–)DART-HRMS temperature-separated MS plots of waste plastic samples.

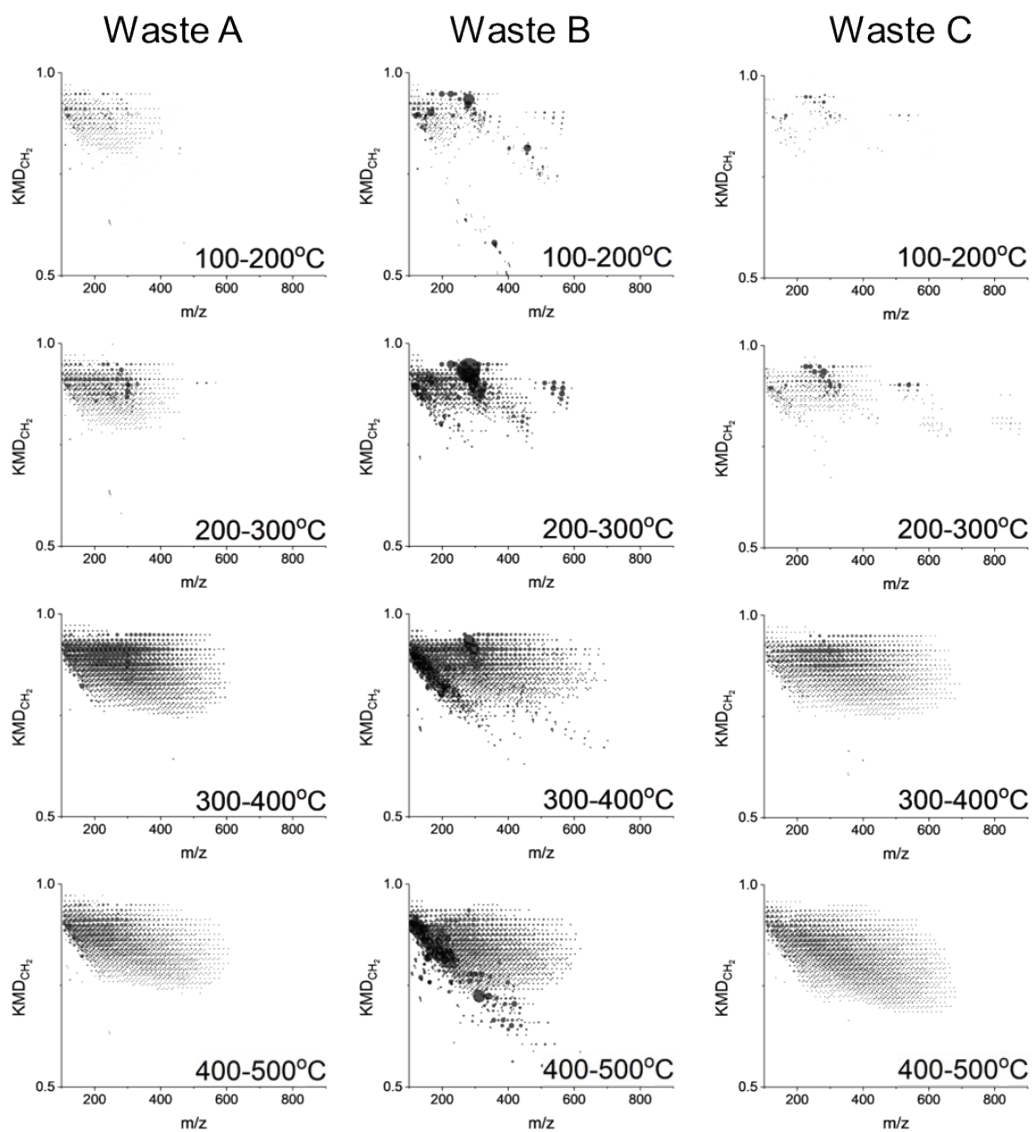


Figure S9: Evolution of CH₂-Kendrick mass defect plots of waste plastics summarized for increasing desorption temperatures in pyro(-)DART-HRMS experiments. Individual points are scaled according to $(\text{intensity})^{1/3}$.

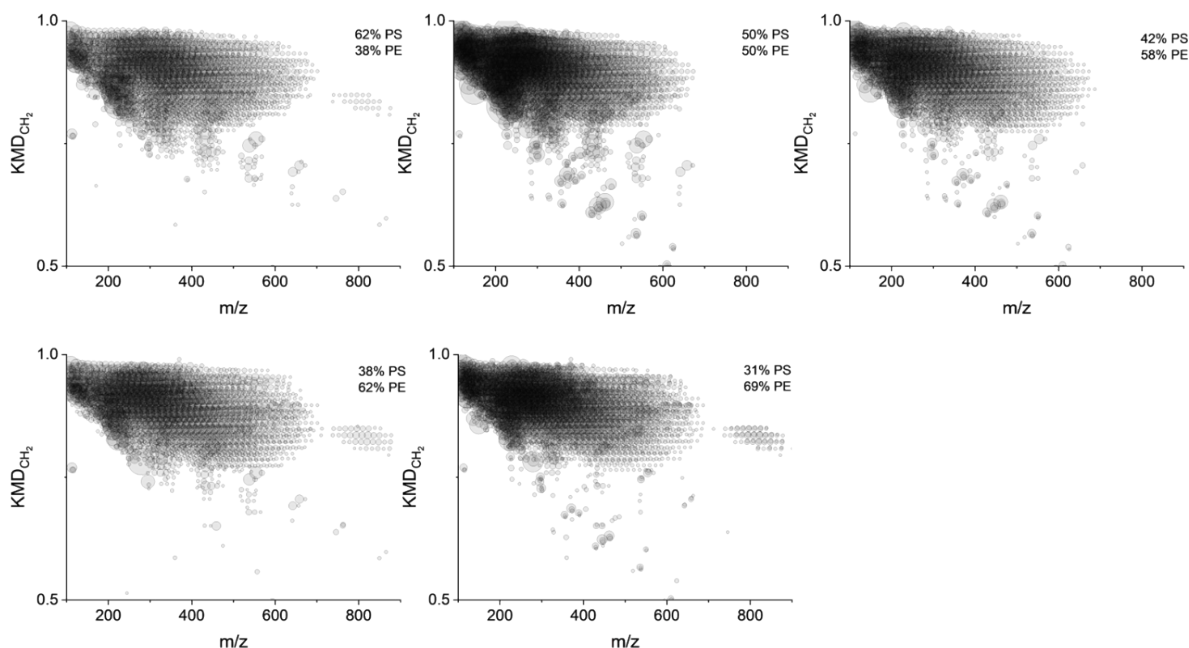


Figure S10: Evolution of CH₂-Kendrick mass defect plots with increasing standard additions of polyethylene to polystyrene. Percentages were determined through weight of analyzed plastic.

Table S1: Results of statistical TC analysis with standard addition mixtures of plastic standards: polyethylene and polystyrene. Increasing percentage of polystyrene increases the similarity score; however, the technique currently does not allow for comprehensive assignment of plastic mixtures.

Plastic Type:	Polyethylene 62% Polystyrene 38%	Polyethylene 50% Polystyrene 50%	Polyethylene 42% Polystyrene 58%	Polyethylene 38% Polystyrene 62%	Polyethylene 31% Polystyrene 69%
Polyethylene	0.22	0.16	0.26	0.55	0.42
Polypropylene	0.14	0.11	0.18	0.34	0.26
Polystyrene	0.11	0.13	0.18	0.21	0.25
Polyvinyl chloride (PVC)	0.03	0.03	0.03	0.03	0.03

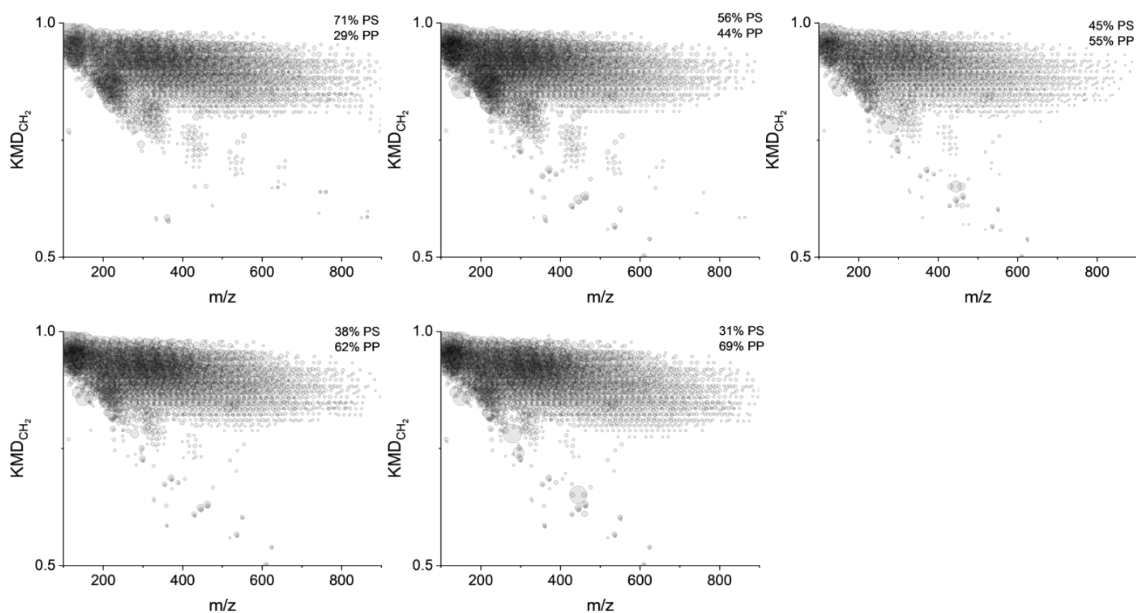


Figure S11: Evolution of CH₂-Kendrick mass defect plots with increasing standard additions of polypropylene to polystyrene. Percentages were determined through weight of analyzed plastic.

Table S2: Results of statistical TC analysis with standard addition mixtures of plastic standards: polyethylene and polystyrene. With plastic mixtures, it becomes difficult to distinguish between polypropylene and polyethylene, and all comparison scores are low.

Plastic Type:	Polypropylene 71% Polystyrene 29%	Polypropylene 56% Polystyrene 44%	Polypropylene 45% Polystyrene 55%	Polypropylene 38% Polystyrene 62%	Polypropylene 31% Polystyrene 69%
Polyethylene	0.15	0.12	0.18	0.30	0.33
Polypropylene	0.12	0.09	0.14	0.25	0.29
Polystyrene	0.06	0.08	0.09	0.12	0.12
Polyvinyl chloride (PVC)	0.02	0.02	0.02	0.03	0.03

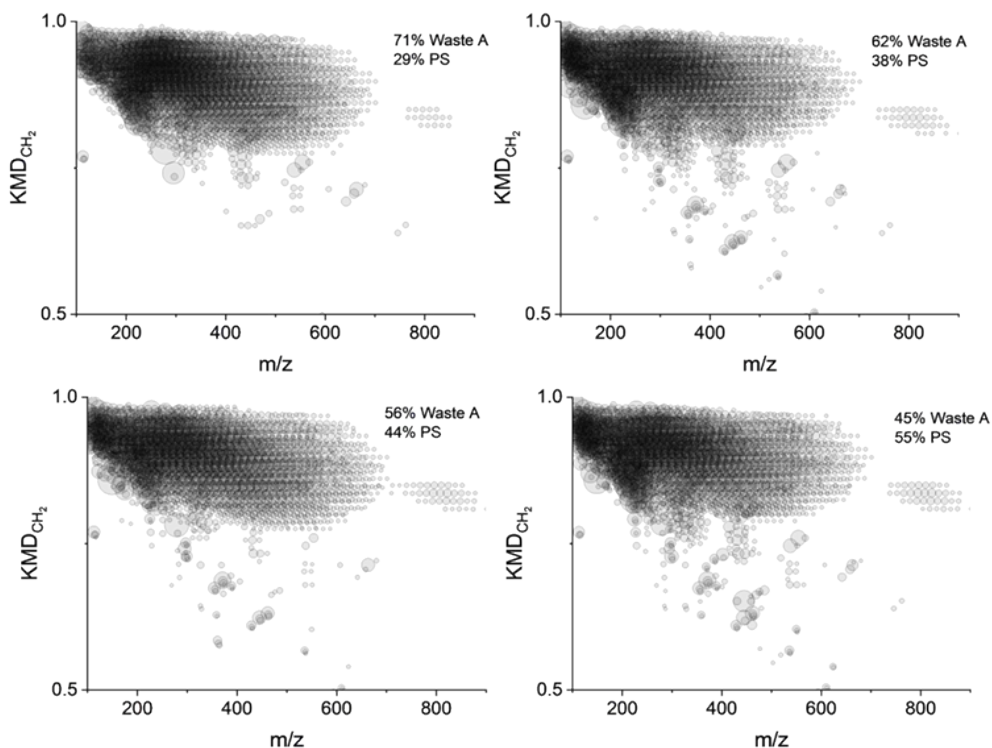


Figure S12: Evolution of CH₂-Kendrick mass defect plots with increasing standard additions of polystyrene to Waste A. Percentages were determined through weight of analyzed plastic.

Table S3: Results of statistical TC analysis with standard addition mixture of plastic standard to plastic waste: polystyrene to Waste A (polyethylene). As more polystyrene is added to the waste, the comparison score drops, illustrating the limitation of the method to assign multi-component plastic mixtures.

Plastic Type:	Waste A 72% Polystyrene 28%	Waste A 62% Polystyrene 38%	Waste A 56% Polystyrene 44%	Waste A 45% Polystyrene 55%
Polyethylene	0.44	0.18	0.44	0.19
Polypropylene	0.29	0.13	0.30	0.13
Polystyrene	0.18	0.10	0.17	0.10
Polyvinyl chloride (PVC)	0.03	0.03	0.03	0.02

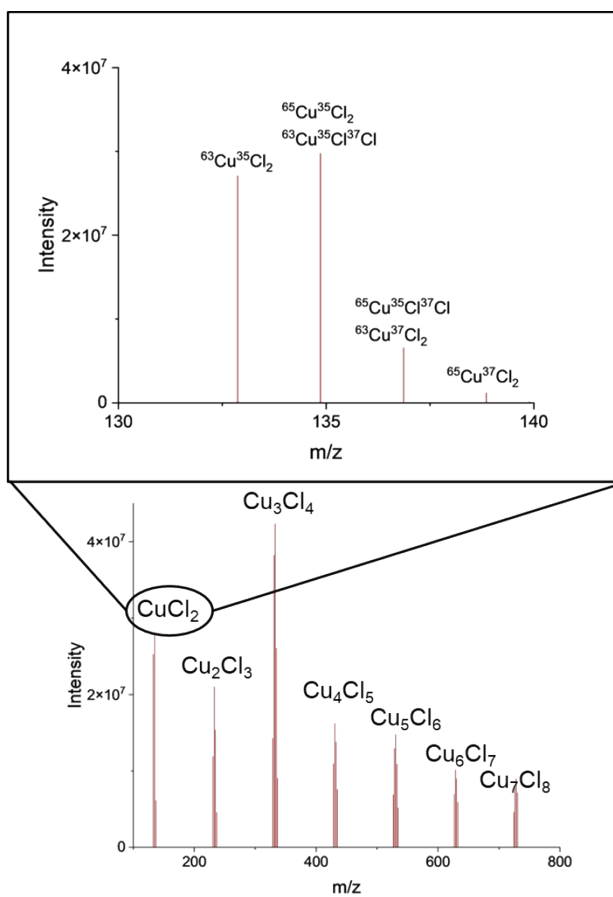


Figure S13: Formula assignments of $\text{Cu}_x\text{Cl}_{x+1}^-$ peaks observed in the PVC pyrolysis products with pyro(-)DART-HRMS.

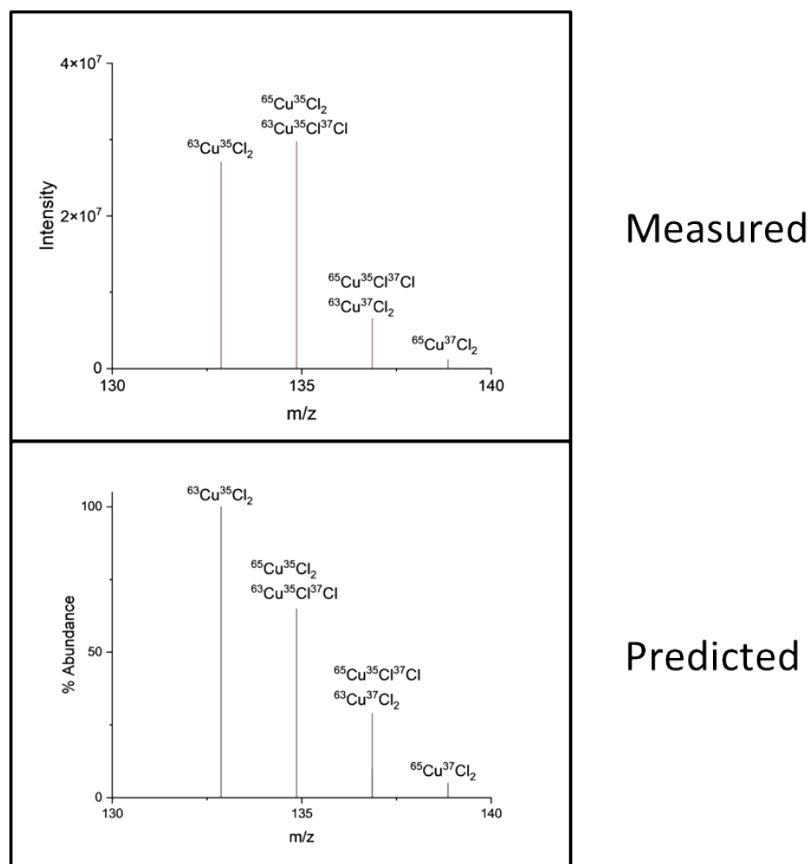


Figure S14: Isotopic distribution of $\text{Cu}_x\text{Cl}_{x+1}^-$ peaks observed in the PVC pyrolysis products with pyro-(–)DART-HRMS, compared to predicted isotope distribution.¹

Appendix A: Description of Tanimoto Coefficient Calculation for one Homologous Series

For each plastic reference standard and the unknown, list of m/z values, intensity values, and corresponding KMD_{CH_2} values are obtained. For a selected KMD value, for example 0.920, a tolerance value (0.001) is applied, and all values within that range (0.919-0.921) from the reference standard datasets and the unknown are grouped.

Table A1: Number of m/z peaks within KMD_{CH_2} 0.919-0.921 for each plastic standard and Waste A.

plastic	m/z count
PE	24
PP	45
PS	12
PVC	1
Waste A	37

The species that fit this range are then normalized within their respective plastic types to avoid skewing related to variations from different masses of measured plastic. The species that fit this specific KMD_{CH_2} range are shown in Fig A1.

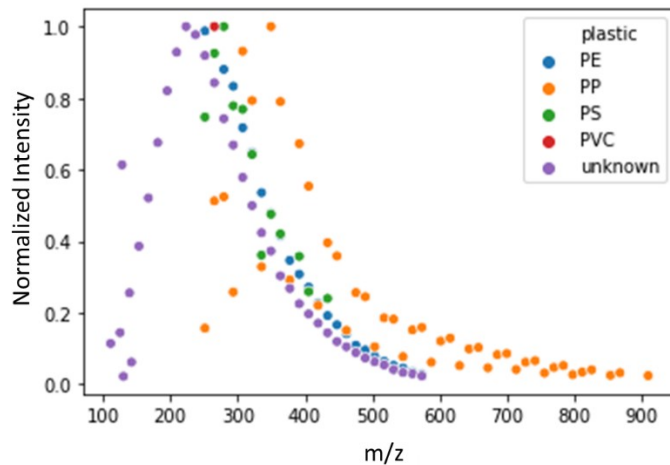


Figure A1: m/z peaks within KMD_{CH_2} 0.919-0.921 for each plastic standard and Waste A (unknown) normalized to 1 within their plastic type.

The m/z values are then binned into groups for comparison between plastic types, such as 100-102, 102-104, and so on. This bin size is chosen to ensure a reasonable number of values for computational comparison, and it is effective for this method. The binned values are depicted in Figure 2A.

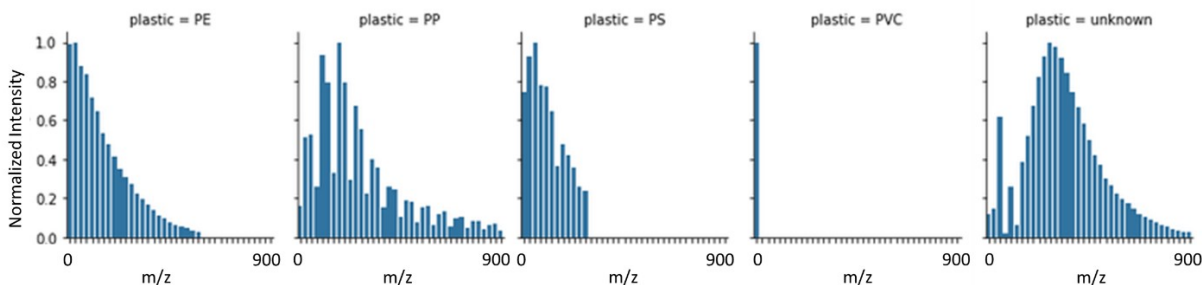


Figure 2A: “Binned” values from plastic standards and Waste A (unknown) between 0.919-0.921.

A Tanimoto similarity score is then calculated for each bin between all plastic types and waste A. The maximum normalized value in each m/z bin, between the unknown and the standard, is considered the union value, as it represents the highest intensity observed in that m/z region. The minimum value in the bin is regarded as the intersection value, representing the lowest or null intensity present.

$$TC(A,B) = \frac{|A \cap B|}{|A \cup B|}$$

For one individual bin (100-102) and for one plastic type (PP vs. Waste A) the calculation would be as follows:

Normalized Intensities: 0.124=Waste A (min), 0.551=Polypropylene (max)

$$TC(PP, \text{Waste A (100-102 } m/z)) = \frac{|0.124|}{|0.551|}$$

$$TC(PP, \text{Waste A (100-102 } m/z)) = 0.23$$

For bins where one of the samples does not have m/z value, the comparison score is zero. The values obtained for each bin are then aggregated by calculating the average score for that homologous series. This process is repeated for all homologous series.

References:

- (1) Manura, J.; Manura, D. Isotope Distribution Calculator and Mass Spec Plotter.